REMOTE SENS. ENVIRON. 42:147–155 (1992)

Enhancement of Multispectral Thermal Infrared Images: Decorrelation Contrast Stretching

Alan R. Gillespie

Department of Geological Sciences, University of Washington, Seattle

Decorrelation contrast stretching is an effective method for displaying information from multispectral thermal infrared (TIR) images. The technique involves transformation of the data to principle components ("decorrelation"), independent contrast "stretching" of data from the new "decorrelated" image bands, and retransformation of the stretched data back to the approximate original axes, based on the inverse of the principle component rotation. The enhancement is robust in that colors of the same scene components are similar in enhanced images of similar scenes, or the same scene imaged at different times. Decorrelation contrast stretching is reviewed in the context of other enhancements applied to TIR images.

INTRODUCTION

Enhancement is the process of adjusting the encoded radiance values in an image with the goal of optimizing the display of information. Enhancement of multispectral thermal infrared (TIR) images of emitted radiation (typically at wavelengths from 8 μm to 14 μm) presents special difficulties, because there is less spectral variation from pixel to pixel, compared to visible/near-infrared (VNIR) images of reflected sunlight (0.4–2.4 μm), and there is a high degree of correlation among the data from different image channels. Nevertheless, several different enhancements—some of them reviewed in companion articles in this volume—have been applied to TIR data successfully (e.g., Gillespie et al., 1986, 1987). One of the most effective techniques, decorrelation contrast stretching (Soha and Schwartz, 1978), is reviewed in this article. The enhancement is illustrated using an image of Death Valley, California, and the results are compared to standard false-color composite and color ratio composites.

Address correspondence to Alan R. Gillespie, Dept. of Geological Sciences, AJ-20, Univ. of Washington, Seattle, WA 98195.

Received 15 July 1992.

0034-4257/92/$5.00

655 Avenue of the Americas, New York, NY 10010

BACKGROUND

Thermal infrared radiance is emitted from a scene as a function of temperature and scene composition. Radiance from an ideal blackbody is exponentially proportional to temperature (Planck's law), which is typically controlled by topography in a terrestrial scene. Although the shape of the blackbody spectrum changes with temperature, the proportion of total radiance at a given wavelength changes negligibly over the range of temperatures common in a typical terrestrial scene. In other words, radiances for this limited range of temperatures lie close to a straight line that

passes close to the origin in a scatter diagram such as Figure 1.

Scene composition influences the emitted TIR radiance via the emissivity spectrum, conceptually similar to reflectivity in the VNIR. The emissivity spectrum modulates the blackbody radiance to produce the measured spectrum. However, emissivity contrast and variability from 8 μm to 14 μm are low, typically $<15\%$ for natural surfaces (e.g., Kahle et al., 1984). The effect on the scene radiance of these small emissivity variations is only about 1% of the variation due to temperature differences. In contrast, reflectivities within a VNIR single spectrum may vary with wavelength by as much as a factor of 5, so that compositional differences may produce nearly the same range of radiance differences as topographic shading from pixel to pixel.

It is the lower contrast in emissivity compared to reflectivity spectra that results in the higher correlation among the different channels of multispectral TIR data, compared to VNIR data. TIR data for many natural surfaces are nearly as linear as the idealized blackbody radiances in the scatter diagram of Figure 1. Multispectral images with this characteristic tend to be virtually colorless when displayed, unless special procedures are invoked during enhancement. Decorrelation stretching, the principal subject of this review, is one of the special procedures that exaggerates the meager color information contained within the image.

Figure 1. Scatter diagram showing the nearly linear relationship between blackbody radiances at 8.5 μm and 10.5 μm, for temperatures commonly encountered in terrestrial scenes (270–370 K). Over a greater range of temperatures, the trajectory of radiance vectors defines a curve.

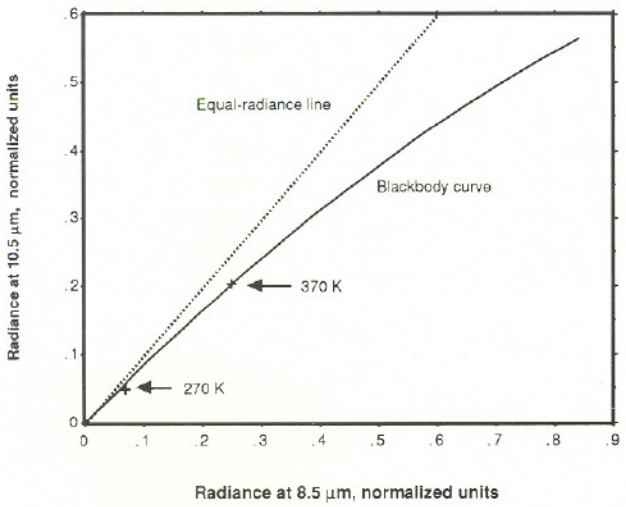

TECHNIQUES

A number of strategies have been used to display the compositional information in TIR data pictorially. These may be divided into three approaches. In the first, the temperature and compositional information that control the measured radiances are enhanced together; in the second, they are mathematically separated before enhancement. The third approach is a hybrid in which the spectral contrast (composition) is boosted without necessarily increasing the range of brightness (temperature), and the equalized information is displayed.

Enhancing Temperature and Composition Data Together

Enhancements using the first approach are probably the most common. Because of the dominance of temperature information, black-and-white images of radiance convey terrain but not composition information. False-color images of three TIR channels convey some compositional information, but the color variations are weakly expressed (Kahle and Rowan, 1980), and even strongly contrast-enhanced color pictures also convey mostly terrain information. Thus simple color compositing—the staple enhancement for VNIR data—is unacceptable for many TIR images.

Enhancing Temperature and Composition Data Separately

Various algorithms, some discussed in companion articles in this volume, have been devised to determine scene emissivity and temperature separately, although the necessary calculations can be complex and involve assumptions that result in a degree of uncertainty. This approach is effective at separating compositional and temperature information, and may be preferred if the goal of analysis is to display temperature information alone.

Separate enhancement has also been used to display compositional information alone. Ratioing

radiance data from different spectral bands is one simple and effective way of suppressing the correlated (temperature) component of the data, while exaggerating the less-correlated (compositional) component. Vincent et al. (1972) demonstrated that a single ratio image of thermal data, created by dividing one image channel by another, enhanced emissivity differences sufficiently to distinguish quartzose sandstone from nonsilicate rocks, and Vincent and Thomson (1972) were able to distinguish dacite from basalt. Color ratio compositing (e.g., Rowan et al., 1974; Crippen, 1987; Gillespie et al., 1987; Crippen et al., 1988) is one approach that allows for the display in a single picture of information from up to six image channels: Combining three different ratio images as the red, green, and blue (*R*, *G*, and *B*) channels of a color picture permits greater discrimination of lithologies than black-and-white displays of single ratio images. However, the colors with which the ratioed data are displayed are of necessity arbitrary, and this makes relating image data and field or laboratory spectra difficult and nonintuitive.

Another way to display compositional data alone involves calculating, from the measured data, emissivities for each image channel. False-color pictures may be made from three individually stretched emissivity images. With the variance due to temperature removed, emissivity data are correlated to roughly the same extent as VNIR data, and in principle the color pictures are effective at conveying information. However, some algorithms used to calculate emissivities also increase image noise to the point where the color pictures can be difficult to interpret (Kahle et al., 1980). One new algorithm (Realmuto, 1990) does not propagate noise from a reference channel and hence produces superior color pictures. Another technique produces emissivity ratio spectra having noise characteristics superior to emissivity spectra themselves (Watson et al., 1990). Log-normal residual algorithms have also been applied (e.g., Hook, 1989; Hook et al., 1990) to solve this problem. However, none of these approaches displays terrain data along with the compositional information.

The loss of context involved in isolating and discarding the temperature information makes interpretation of the compositional information more difficult. Photointerpretation is facilitated by displaying the compositional and terrain information together, but equally well. The hybrid approaches that seek to increase the spectral contrast, without exaggerating the pixel-to-pixel lightness variations, were devised to solve this problem.

Hybrid Enhancements

One hybrid enhancement involves recombining in a controlled way the separately enhanced emissivity and temperature data. For example, it is possible to modulate ratio pictures of VNIR images, substantially free of terrain information, by the albedo image to add back the geographic context [for a different technique see Crippen et al. (1988)]. This has also been done for TIR images (Gillespie et al., 1987). Separately enhanced emissivity and temperature images may be recombined, simply by multiplying the different emissivity images by the common temperature image and rescaling the product for display.

Various coordinate transformations (e.g., hue–saturation–intensity, or HSI) have been used to enhance color information directly, without first calculating emissivities and temperature explicitly (Gillespie et al., 1986; 1987). These procedures exaggerate color saturation, while preserving the same hues found in a simple radiance false-color picture. They require transformation to another domain in which contrast stretching is applied, followed by retransformation to the original domain for display. Perhaps the simplest and most effective of this category of enhancement is based upon the principal component (PC) transformation. The PC approach is known as "decorrelation stretching" (Soha and Schwartz, 1978; Kahle and Rowan, 1980; Gillespie et al., 1986).

DECORRELATION STRETCHING

To display highly correlated thermal images as colorful pictures, it is necessary to exaggerate the least correlated part of the information selectively. This corresponds to exaggerating color saturation independent of lightness. Decorrelation stretching accomplishes this while leaving the distribution of hues substantially unmodified, for most TIR images.

Decorrelation stretching is accomplished in

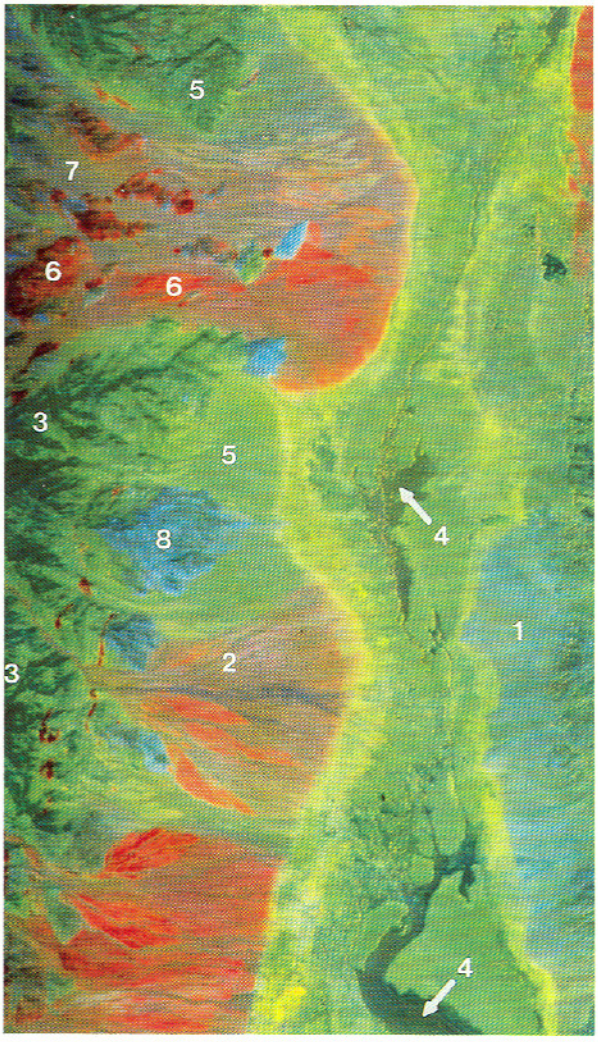

(a)

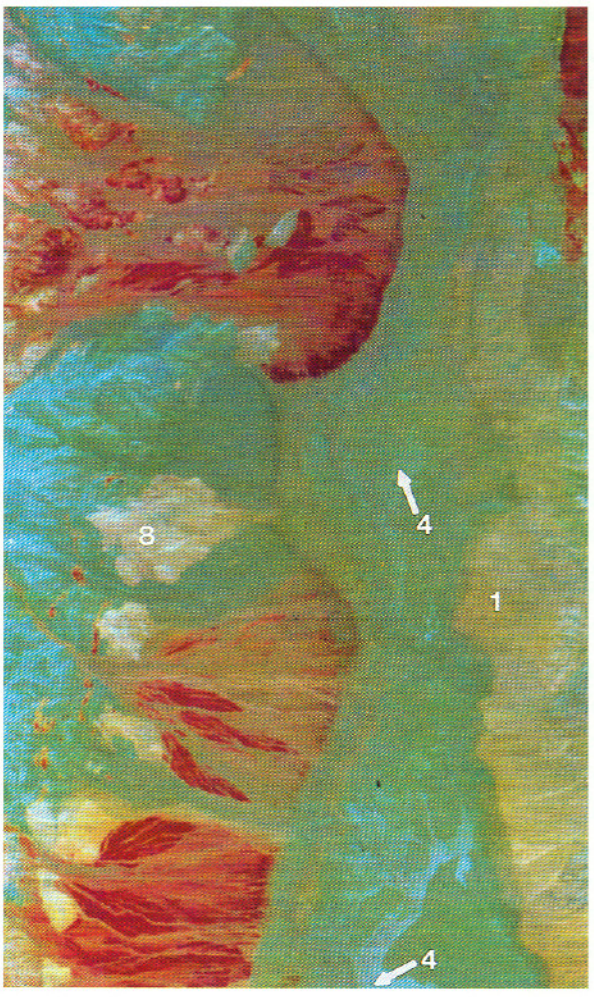

(b)

four steps. In the first step, the covariance matrix is determined for the image and the eigenvectors are calculated. In the second step, the image is actually transformed from the radiance domain to the PC space. The PC transformation is described by Gonzales and Wintz (1977). It is just a special linear transformation (rotation and translation) of the radiance space, but the transformed data have the unique property that they are statistically independent or "decorrelated." In the third step, the PC images are separately contrast-stretched, generally to equalize the variances of the three or more images with the highest signal-to-noise ratios. In the fourth step, the inverse transformation is calculated that would rotate the unstretched PC images back to the original radiance space, and this transformation is applied to the stretched data. Even though the data are retransformed to the radiance space, the covariance of the enhanced images is reduced. Three of the retransformed image channels are displayed as a false-color picture.

Experience has shown that a wide range of scenes imaged by NASA's TIMS (Palluconi and Meeks, 1985) and other TIR scanners have roughly similar covariance matrices, and the enhancements are more consistent than expected from the inherent individuality of the PC transformation. In general, the hues of the enhanced picture are similar to the hues before decorrelation stretching, but the saturations are increased.

Stretched PC images themselves have been arbitrarily assigned to *R*, *G*, and *B* for display. Although this approach produces colorful pictures, relating the display colors to emissivity spectra is not straightforward. Transforming the enhanced PC images back to the original coordinates overcomes this deficiency, and interpretation of the enhanced images is simpler.

Because it is based upon PC analysis, decorre-

(c)

Figure 2. Three enhanced versions of a TIR image of Death Valley, California, acquired by NASA's TIMS scanner near noon on 27 August 1982. TIMS acquires data in six bands centered at wavelengths 8.3 μm, 8.7 μm, 9.1 μm, 9.8 μm, 10.4 μm, and 11.3 μm (Palluconi and Meeks, 1985). North is up, the image is ~25 km from top to bottom. The nadir ground pixel size is ~18 m. The data were nominally calibrated, scan by scan, using dual onboard blackbody measurements, and geometrically resampled to rectify scan-angle foreshortening. Both the above corrections were done at the Jet Propulsion Laboratory. a) Standard false-color composite, with R, G, and B = Channels 5, 3, and 1, enhanced by stretching radiance data only; b) color ratio composite, with R, G, and B = Channels 5 / 4, 3 / 4, and 1 / 4; c) decorrelation-stretched image, with R, G, and B = Channels 5, 3, and 1 (JPL Photo # P-26340).

lation stretching is readily extended from the three image channels needed for color compositing to any number of image channels. This feature is not shared with otherwise comparable enhancements, such as the one based on the HSI transformation. The generality of PC analysis is useful if color pictures of different triplets of channels from the same image are to be compared. On the other hand, it is not feasible to display information from more than three channels at a time; for that it is necessary to use spectral identification or characterization routines (e.g., Clarke et al., 1990; Gillespie and Abbott, 1984), or spectral mixture analysis (e.g., Adams et al., 1986; Gillespie et al., 1990a,b; Smith et al., 1990).

EXAMPLE

Figure 2 shows three false-color pictures from part of a six-channel TIMS image of Death Valley, California. Death Valley is complex lithologically, and sparsely vegetated. It has been studied previously using multispectral thermal images (Kahle and Goetz, 1983; Kahle et al., 1984; Gillespie et al., 1984). Figures 2a, b, and c were each enhanced differently, by: linear contrast stretching of each channel independently (Fig. 2a); ratioing to a common denominator channel (Fig. 2b); and decorrelation stretching (Fig. 2c). Important features in the scene are numbered in Figure 2a. The image spans Death Valley itself and includes the adjacent piedmonts (1, 2) as well as part of the Panamint range (3). On the valley floor shallow standing water (4), calcite, halite, and silty sediments dominate. The eastern piedmont contains volcanic and gneissic gravels. The Panamints and the western piedmont are largely dolomite (5) and quartzite (6), with lesser volumes of shale (7) and volcanic rocks (8). Vegetation is generally sparse. The mountains support a piñon-juniper woodland above creosote-bush plains. The valley floor is unvegetated.

The false-color composite (Fig. 2a) was made

by assigning the primary colors (RGB) to TIMS Channels 5, 3, and 1 in order of descending wavelength, which facilitates comparison to laboratory spectra. Nevertheless, Figure 2a contains relatively pallid or unsaturated colors. In Figure 2a, quartzites appear red, shales purple, volcanic rocks blue, and carbonates, vegetation, and evaporites are greenish. Standing water on the valley floor (4) is also green, and dark because evaporative cooling has lowered its surface temperature. All these colors are readily interpreted in terms of the emissivity spectra of the different surface materials (Kahle and Goetz, 1983), once it is understood that spectrally flat materials (e.g., dolomite, vegetation) are represented as green instead of gray, and that all other colors are similarly shifted.

The Death Valley data have an unusually high range of emissivity contrasts, compared to most scenes. In part, this due to the sparse cover of vegetation in the scene, but it is also due to the range of lithologies—especially quartzite, which has a strong Si—O reststrahlen bands (and hence strong spectral contrast) in the TIMS spectral window (Lyon, 1965; Hunt and Salisbury, 1974; 1975; 1976).

Figure 2b is a color ratio composite made using the same three TIMS channels from Figure 2a (centered at 10.4 μm, 9.1 μm, and 8.3 μm) as numerators, each normalized to the same denominator channel (9.8 μm). The hues of the image are substantially the same as in Figure 2a, except that the volcanic rocks (8) and the gneissic rocks of the eastern piedmont (1) appear pink instead of blue. In general, the color saturations in Figure 2b are increased, and the intensity (light / dark) contrasts are lessened, relative to Figure 2a. However, there are also some striking differences in intensity values. This is especially noticeable where there is standing water on the valley floor (4), dark in Figure 2a but light in the color ratio composite. The cool ridgetops of the Panamints are likewise light in the ratio image. This residual topographic information in the ratio images has been attributed to incomplete removal of atmospheric scattering or instrument effects from the data (Podwysocki et al., 1984; Gillespie et al., 1987).

To create Figure 2c, PC analysis of all six channels was performed in one step, after which the variances along PC axes 2–4 (decreasing eigenvalues) were increased to equal the variance along PC axis 1 (largest eigenvalue). No stretch was applied to PC axes 5 and 6, which were dominated by striping and other image noise. The inverse PC transformation was then applied to recreate six enhanced radiance images. The same triplet of channels used in Figure 2a was selected for display.

Figures 2c and 2a have similar hues, but the saturations in the decorrelation-stretched image are greater. The sense and strength of intensity variations is unchanged from Figure 2a. Quartzose rocks appear red; the volcanic and gneissic rocks are purple; and vegetation and carbonate rocks, both of which lack emissivity contrast in this window, are displayed as green, because the decorrelation algorithm forces the average color of the image towards gray. Spectrally flat evaporites such as halite, in the center of the valley, also appear green. However, the increased saturation reveals a yellowish rind around the valley floor that appears to be a zone enriched in gypsum (Hunt and Mabey, 1966). This zone appeared light green in Figure 2a.

Figure 3 shows cluster diagrams for DN pairs from each picture in Figure 2. The chief points these clusters illustrate are (1) the high degree of elongation for the false-color composite (Fig. 3a) and (2) the more equant clusters for the ratio and decorrelation-stretched images (Figs. 3b and c). Figure 3a contains essentially two elongate clusters. The upper cluster corresponds to the spectrally neutral scene components; the lower cluster corresponds to the quartzites. The elongation along the main diagonal of the plane is attributable to the range of temperatures at which the scene components are imaged.

Figure 3b displays the cluster diagram for the ratio image. Radiance data lying on straight lines passing through the origin of Channel 5 vs. 4 and 3 vs. 4 planes similar to Figure 3a will plot as points in Figure 3b. If the lines do not include the origin, the data in Figure 3b will plot in a diffuse cluster. The systematically high 5 / 4 and 3 / 4 ratio values for cool scene elements indicated in the ratio picture (Fig. 2b) probably result from this cause. The data in Figure 3b lie in two clusters, as was the case for Figure 3a. The significance of the clusters is the same in both diagrams.

Figure 3c displays the cluster diagram for the decorrelation-stretched image. The diagram

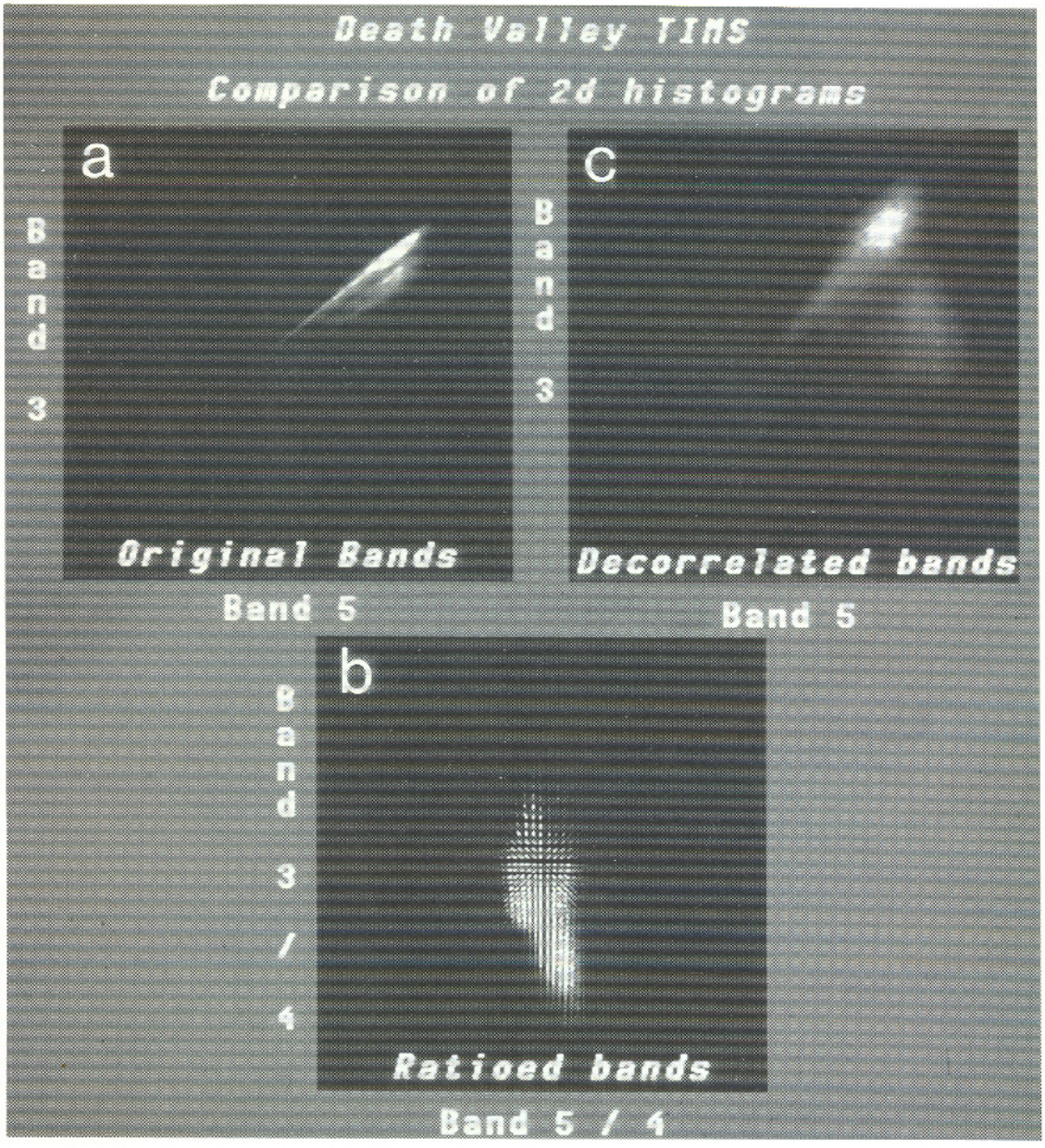

Figure 3. Two-dimensional clusters of data pairs for the three enhanced versions of the Death Valley image of Figure 2: a) standard false-color enhancement, Channels 5 and 3; b) ratio data, Channels 5 / 4 and 3 / 4; c) decorrelation-stretched data, Channels 5 and 3.

resembles Figure 3a, except that the two clusters have been expanded perpendicular to the direction of their original elongation by the enhancement. This is one graphical representation of the wider range of saturated hues in Figure 2c.

A line fitted to the upper cluster in Figure 3c would not be parallel to an equivalent line in Figure 3a. This discordance is not inherent in the decorrelation procedure, but resulted because the covariance matrix was determined for a subset of the image only, as a matter of convenience. The discordance apparently occurred because the principle axis of the subset data was not aligned with the principle axis of the entire image. Thus, when the variances were equalized, the principle axis of the image was rotated.

CONCLUDING COMMENTS

Figure 2c demonstrates the retention of both terrain and compositional information in a single

decorrelation-stretched picture. However, in order to display all the compositional information contained in the multispectral image, it would be necessary to construct several versions using different channels. For six-channel scanners such as TIMS, this may not be an insurmountable obstacle, but for thermal imaging spectrometers envisioned for the future, analogous to the existing VNIR AIS and AVIRIS instruments, it will be necessary to extract mineralogical information from all channels at once. This is beyond the reach of simple enhancement techniques. Even so, decorrelation stretching may continue to be useful in providing pictures for survey or first-look analysis.

Research support was from NASA's Solid Earth Sciences Branch and EOS program. Jack Salisbury provided a helpful review. Assistance of the Jet Propulsion Laboratory is appreciated.

REFERENCES

Adams, J. B., Smith, M. O., and Johnson, P. E. 1986. Spectral mixture modeling: A new analysis of rock and soil types at the Viking Lander 1 site. *J. Geophys. Res.* 91:8098–8122.

Clarke, R. N., Gallagher, A., and Swayze, G. A. 1990. Material absorption band depth mapping of imaging spectrometer data using a complete band shape least-squares fit with library reference spectra. *Proc. 2nd Airborne Visible/Infrared Imaging Spectrometer (AVIRIS) Workshop*, JPL Publ. 90–54, Jet Propulsion Laboratory, Pasadena, CA, pp. 176–186.

Crippen, R. E., 1987. The regression intersection method of adjusting image data for band ratioing. *Internat. Jour. Remote Sens.* 8:137–155.

Crippen, R. E., Blom, R. G., and Heyada, J. R. (1988), Directed band ratioing for the retention of perceptually-independent topographic expression in chromaticity-enhanced imagery, *Int. J. Remote Sens.* 9:749–765.

Gillespie, A. R., and Abbott, E. A. (1984), Mapping compositional differences in silicate rocks with six-channel thermal images, in *Proc. 9th Canadian Symp. Remote Sens.*, St. John's, Newfoundland, Canada, 14–17 August, pp. 327–336.

Gillespie, A. R., Kahle, A. B., and Palluconi, F. D. (1984), Mapping alluvial fans in Death Valley, California, using multichannel thermal infrared images, *Geophys. Res. Lett.* 11:1153–1156.

Gillespie, A. R., Kahle, A. B., and Walker, R. E. (1986), Color enhancement of highly correlated images. I. Decorrelation and HSI contrast stretches, *Remote Sens. Environ.* 20:209–235.

Gillespie, A. R., Kahle, A. B., and Walker, R. E. (1987), Color enhancement of highly correlated images. II. Channel ratio and chromaticity transformation techniques, *Remote Sens. Environ.* 22:343–365.

Gillespie, A. R., Smith, M. O., Adams, J. B., and Willis, S. C. (1990a), Spectral mixture analysis of multispectral thermal infrared images, in *Proc. 2nd Thermal IR Multispectral Scanner (TIMS) Workshop*, JPL Publ. 90–55, Jet Propulsion Laboratory, Pasadena, CA, pp. 57–74.

Gillespie, A. R., Smith, M. O., Adams, J. B., and Willis, S. C. (1990b), Spectral mixture analysis of multispectral thermal infrared images: two test cases, in *Proc. 5th Australasian Remote Sens. Conf.*, Perth, Australia, 8–12 October, Vol. 1, pp. 381–390.

Gonzales, R. C., and Wintz, P. (1977), *Digital Image Processing*, Addison-Wesley, Reading, MA, pp. 103–112 and 309–317.

Hook, S. J. (1989), An evaluation of NS001 and TIMS data for lithological mapping and mineral exploration in weathered vegetated terrain, Ph.D. dissertation, University of Durham, England, 306 pp.

Hook, S. J., Gabell, A. R., Green, A. A., Kealy, P. S., and Kahle, A. B. (1990), A comparison of the model emittance, thermal log residual and alpha residual techniques using TIMS data acquired over Cuprite, Nevada, in *Proc. 2nd Thermal IR Multispectral Scanner (TIMS) Workshop*, JPL Publ. 90–55, Jet Propulsion Laboratory, Pasadena, CA, pp. 17–25.

Hunt, C. B., and Mabey, D. R. (1966), Stratigraphy and structure, Death Valley, California. U. S. Geol. Survey Professional Paper 494-A, 162 pp.

Hunt, G. R., and Salisbury, J. W. (1974), Mid-infrared spectral behavior of sedimentary rocks, U.S. Air Force Cambridge Research Laboratories Technical Report AFCRL-TR-74-0625.

Hunt, G. R., and Salisbury, J. W. (1975), Mid-infrared spectral behavior of igneous rocks, U.S. Air Force Cambridge Research Laboratories Technical Report AFCRL-TR-75-0376.

Hunt, G. R., and Salisbury, J. W. (1976), Mid-infrared spectral behavior of metamorphic rocks, U.S. Air Force Cambridge Research Laboratories Technical Report AFCRL-TR-76-0003.

Kahle, A. B., and Goetz, A. F. H. (1983), Mineralogic information from a new airborne thermal infrared multispectral scanner, *Science* 222:24–27.

Kahle, A. B., and Rowan, L. C. (1980), Evaluation of multispectral middle infrared images for lithologic mapping in the East Tintic mountains, Utah, *Geology* 8:234–239.

Kahle, A. B., Madura, D. P., and Soha, J. M. (1980), Middle infrared multispectral aircraft scanner data: analysis for geological applications, *Appl. Opt.* 19:2279–2290.

Kahle, A. B., Shumate, M. S., and Nash, D. B. (1984), Active airborne infrared laser system for identification of surface rocks and minerals, *Geophys. Res. Lett.* 11:1149–1152.

Lyon, R. J. P. (1965), Analysis of rocks by spectral infrared emission (8 to 25 microns), *Econ. Geol.* 60:715–736.

Palluconi, F. D., and Meeks, G. R. (1985), *Thermal Infrared Multispectral Scanner (TIMS): An Investigator's Guide to TIMS Data*, JPL Publication 85-32, Jet Propulsion Laboratory, Pasadena, CA.

Podwysocki, M. H., Power, M. SD., Salisbury, J. W., and Jones, O. D. (1984), Evaluation of low-sun illuminated Landsat-4 Thematic Mapper data for mapping hydrothermally altered rocks in southern Nevada, in *Proc. Third Thematic Conference, Remote Sens. in Exploration Geology*, Colorado Springs, CO, 16–19 April, pp. 541–551.

Realmuto, V. J. (1990), Separating the effects of temperature and emissivity: Emissivity spectrum normalization, in *Proc. 2nd Thermal IR Multispectral Scanner (TIMS) Workshop*, JPL Publ. 90–55, Jet Propulsion Laboratory, Pasadena, CA, pp. 31–36.

Rowan, L. C., Wetlaufer, P. H., Goetz, A. F. H., Billingsley, F. C., and Stewart, J. H. (1974), Discrimination of hydrothermally altered areas and rock types using computer enhanced ERTS images, south central Nevada, *U. S. Geol. Survey Prof. Paper* 883, 35 pp.

Smith, M. O., Ustin, S. L., Adams, J. B., and Gillespie, A. R. (1990), Vegetation in deserts: I. A regional measure of abundance from multispectral images, *Remote Sens. Environ.* 31:1–26.

Soha, J. M., and Schwartz, A. A. (1978), Multispectral histogram normalization contrast enhancement, in *Proc. 5th Canadian Symposium on Remote Sens.*, Victoria, BC, Canada, pp. 86–93.

Vincent, R. K., and Thomson, F. J. (1972), Rock type discrimination from ratioed infrared scanner images of Pisgah Crater, California, *Science* 175:986.

Vincent, R. K., Thomson, F., and Watson, K. (1972), Recognition of exposed quartz sand and sandstone by two-channel infrared imagery, *J. Geophys. Res.* 77:2473–2477.

Watson, K., Kruse, F. A., and Hummer-Miller, S. (1990), Thermal infrared exploration in the Carlin trend, northern Nevada, *Geophysics* 55:70–79.